BEILSTEIN JOURNAL OF NANOTECHNOLOGY

Supporting Information

for

Upcycling of polyurethane waste by mechanochemistry: synthesis of N-doped porous carbon materials for supercapacitor applications

Christina Schneidermann, Pascal Otto, Desirée Leistenschneider, Sven Grätz, Claudia Eßbach and Lars Borchardt

Beilstein J. Nanotechnol. **2019,** *10,* 1618–1627. doi:10.3762/bjnano.10.157

Materials and methods, additional figures and activation mechanism

Contents

S1 Materials and Methods

The polyurethane foam was purchased from SOUDAL. Urea and K_2CO_3 were purchased from Grüssing GmbH. All chemicals were used without further purification.

Scanning electron microscopy (SEM) was carried out using a Hitachi SU 8020 at a beam voltage of 2 kV.

Thermogravimetric analysis (TGA) was performed on a Netzsch STA 409 PC/PG system using alumina crucibles under argon stream with a heating rate of 10 °C·min^{-1}.

X-ray diffraction (XRD) measurements were performed on a Xpert Pro from PANalytical using Cu Kα_1 (λ = 1.54056 Å) radiation as five-fold determination in the 2θ range of 5–70° with a step width of 0.026. The received X-ray diffractograms were compared with the Inorganic Crystal Structure Database (ICSD) regarding position and intensity of the reflections.

S2 Figures

S2.1 IR spectra

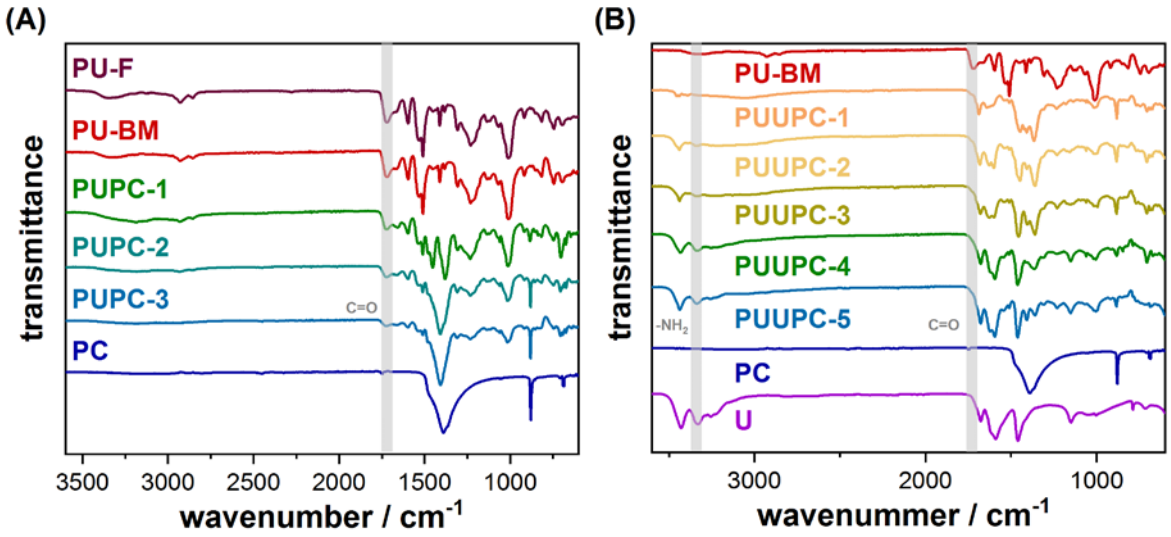

Figure S1: (A) Infrared-spectra of PU foam (PU-F) compared with PU ball-milled (PU-BM) with different amounts of K_2CO_3 (PUPC) and (B) PU-BM compared with PU milled with different amounts of K_2CO_3 and urea (PUUPC).

S2.2 XRD

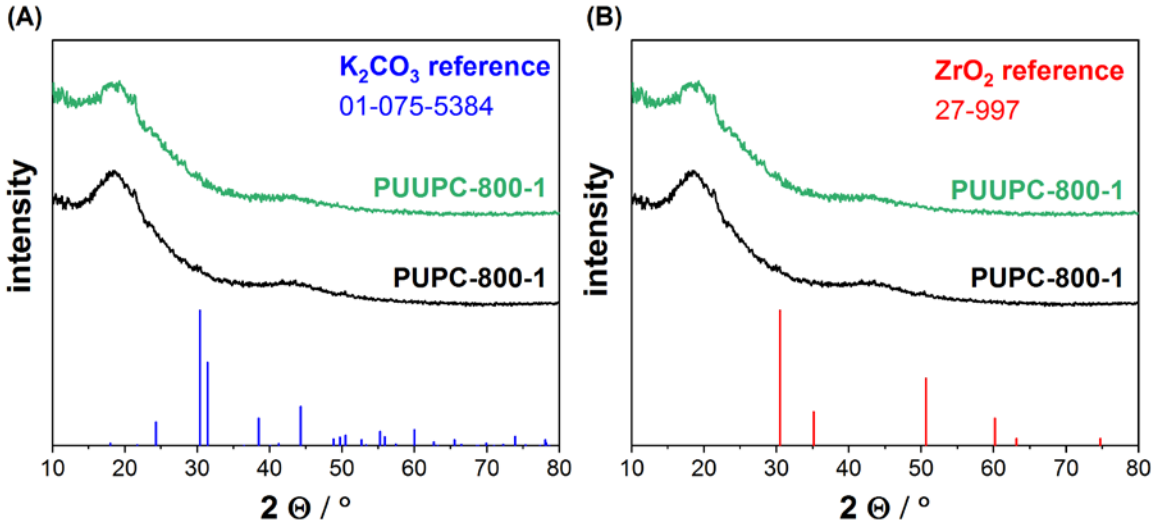

Figure S2: X-ray diffractograms of PUUPC-800-1 (green) and PUPC-800-1 (black) with K_2CO_3 reference (A/blue) and ZrO_2 reference (B/red).

S2.3 SEM

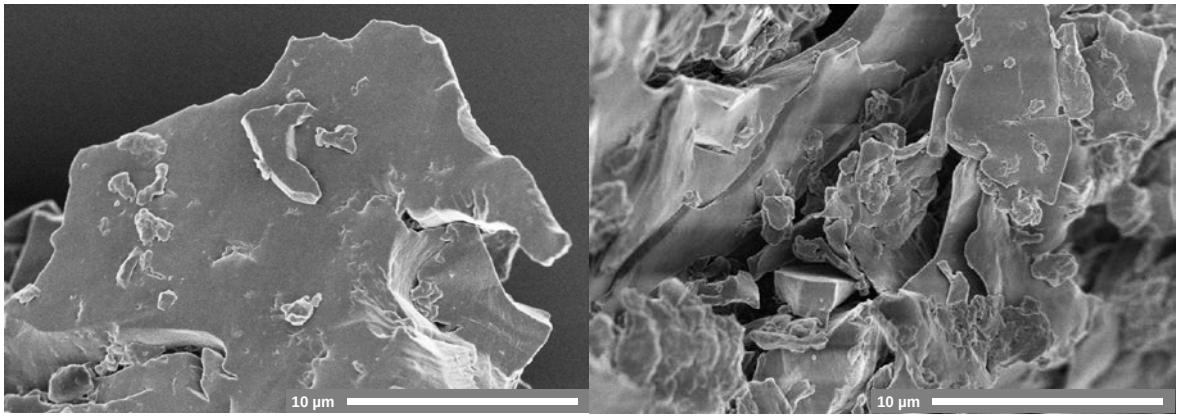

Figure S3: SEM images of PU-BM before pyrolysis.

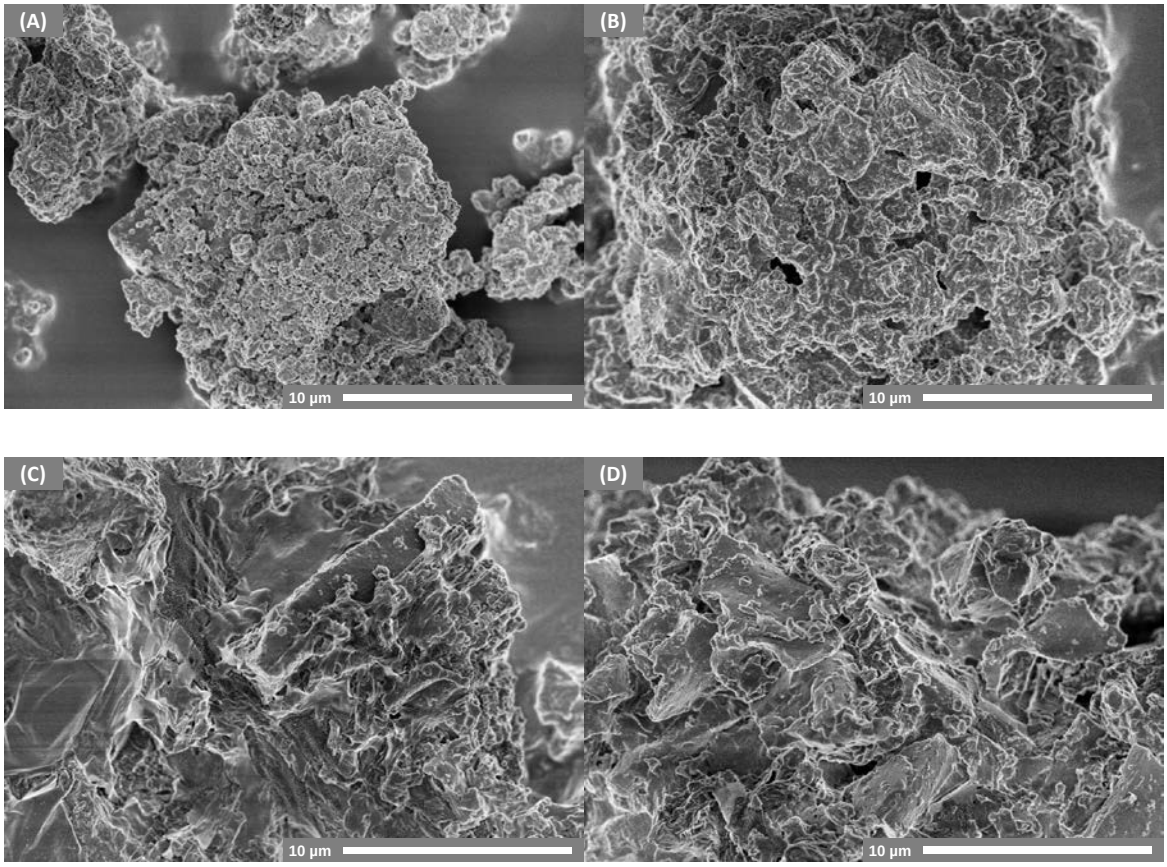

Figure S4: SEM pictures of PUPC-3 (A), PUUPC-1 (B), PUUPC-2 (C) and PUUPC-3 (D) before pyrolysis.

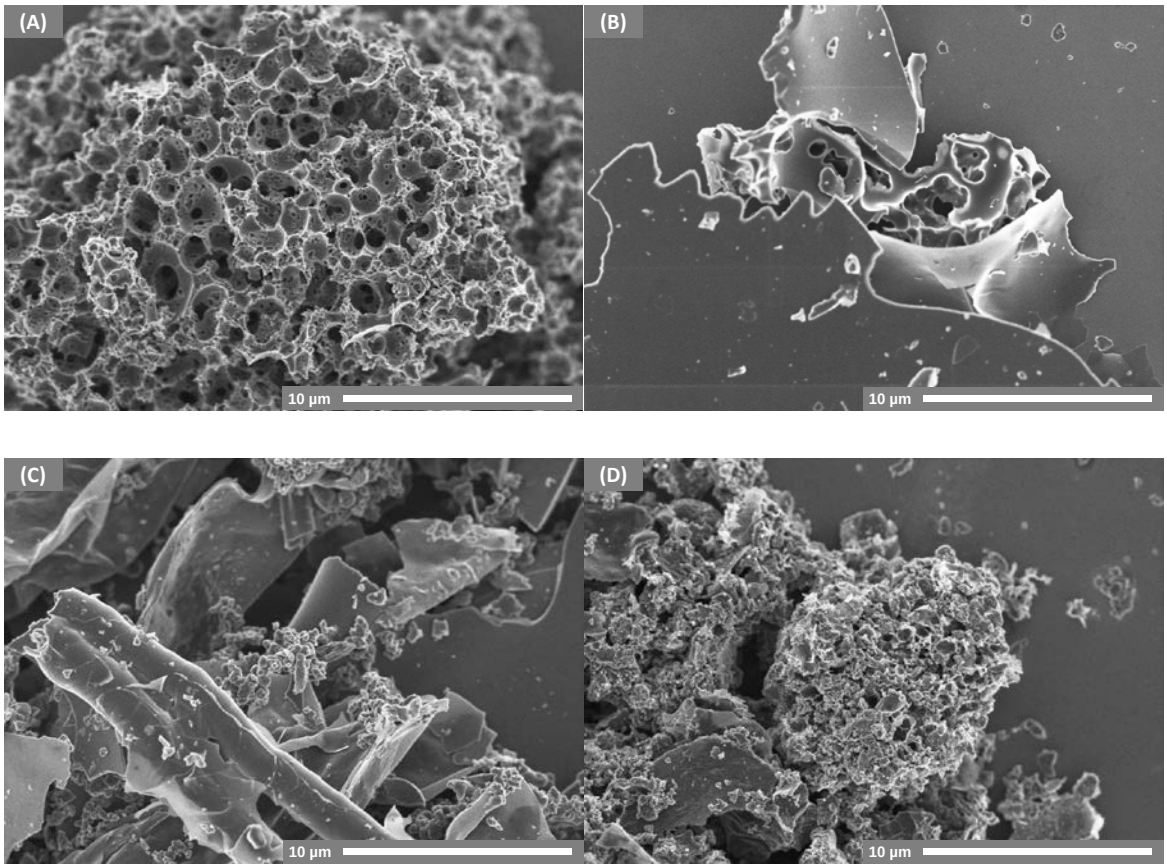

Figure S5: SEM pictures of the samples PUPC-3-800 (A), PUUPC-1-800 (B), PUUPC-2-800 (C) and PUUPC-3-800 (D).

S2.4 TGA

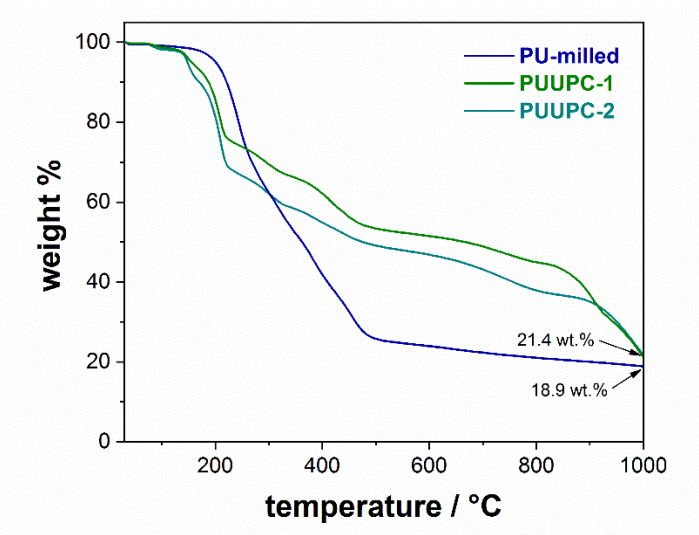

Figure S6: Thermogravimetric analysis of the samples PU-BM (blue), PUUPC-1 (green) and PUUPC-2 (cyan).

S2.5 Dynamic contact angle measurements

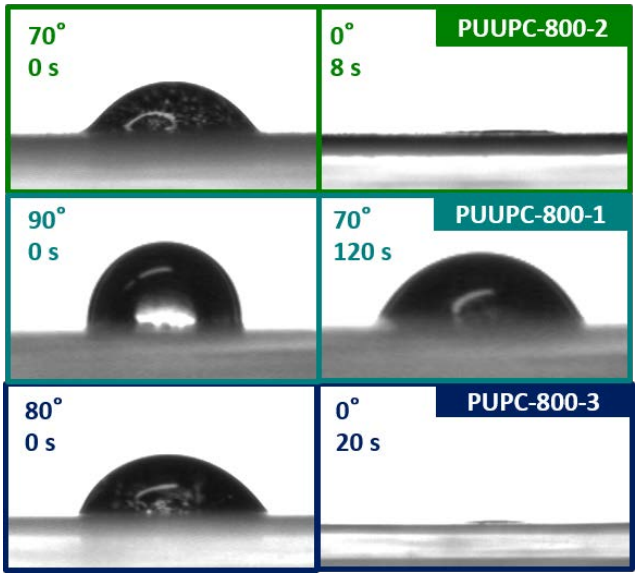

Figure S7: Dynamic contact angle measurements of the samples PUUPC-800-2 (green), PUUPC-800-1 (cyan) and PUPC-800-3 (blue).

S2.6 Conductivity measurements

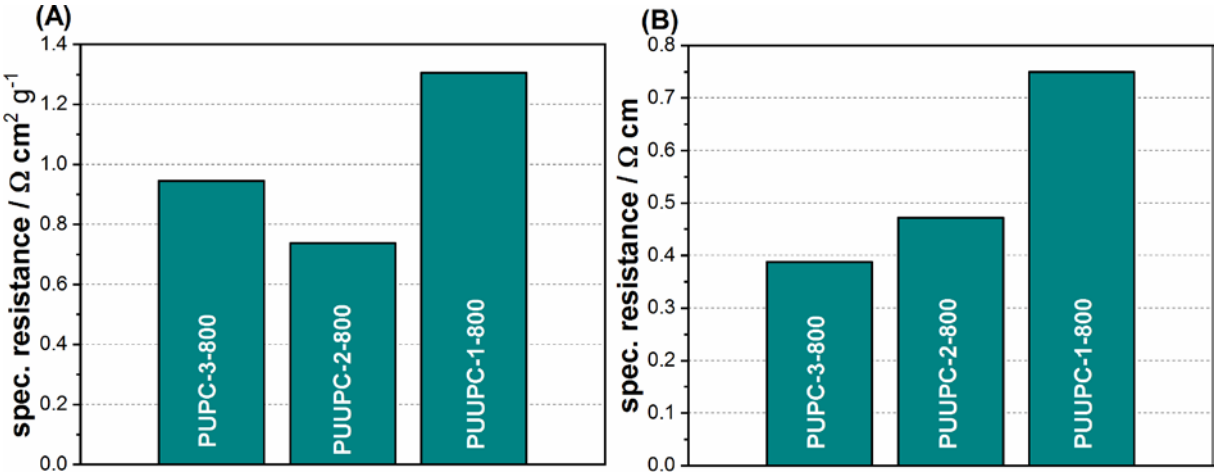

Figure S8: Powder conductivities. Gravimetric (A) and normalized (B) to the surface of electrode (d = 1 cm) for the samples PUPC-3-800, PUUPC-2-800 and PUUPC-1-800.

S2.6 Electrochemical characterization

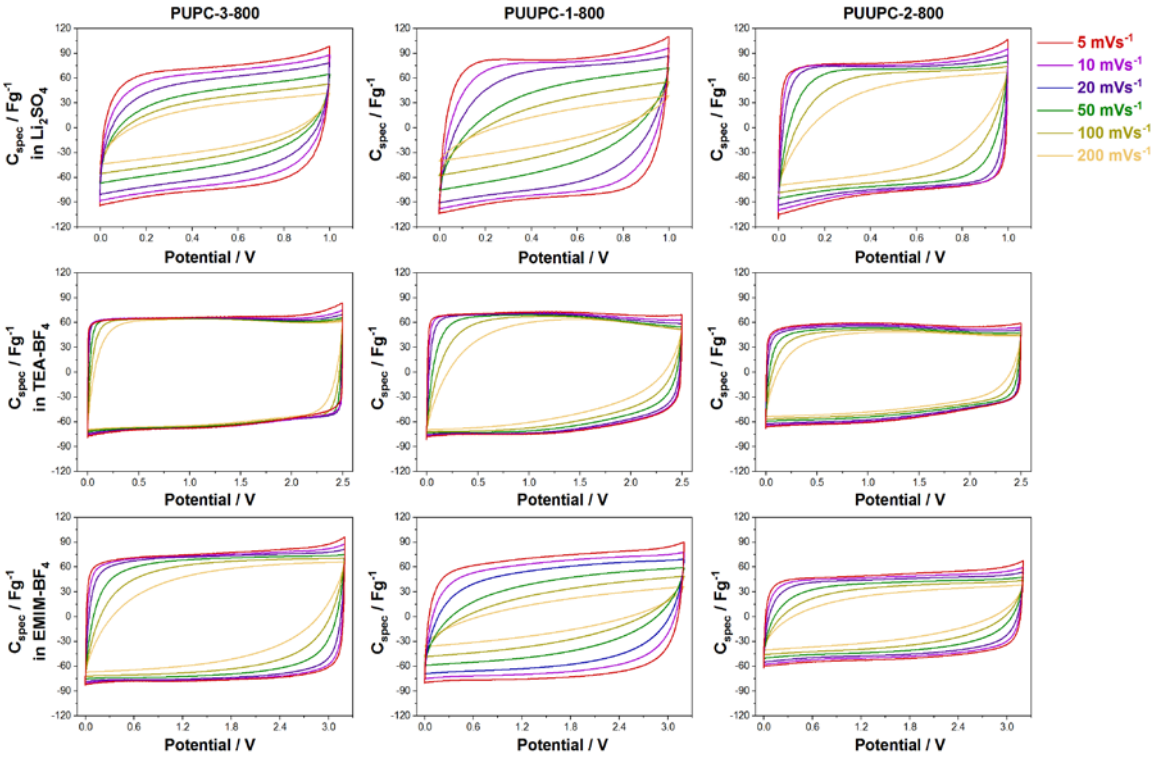

Figure S9: Cyclic voltammetry (CV) matrix of samples PUPC-3-800, PUUPC-1-800, and PUUPC-2-800 measured in aqueous electrolyte Li_2SO_4, organic electrolyte TEA-BF_4 in ACN and ionic electrolyte EMIM-BF_4.

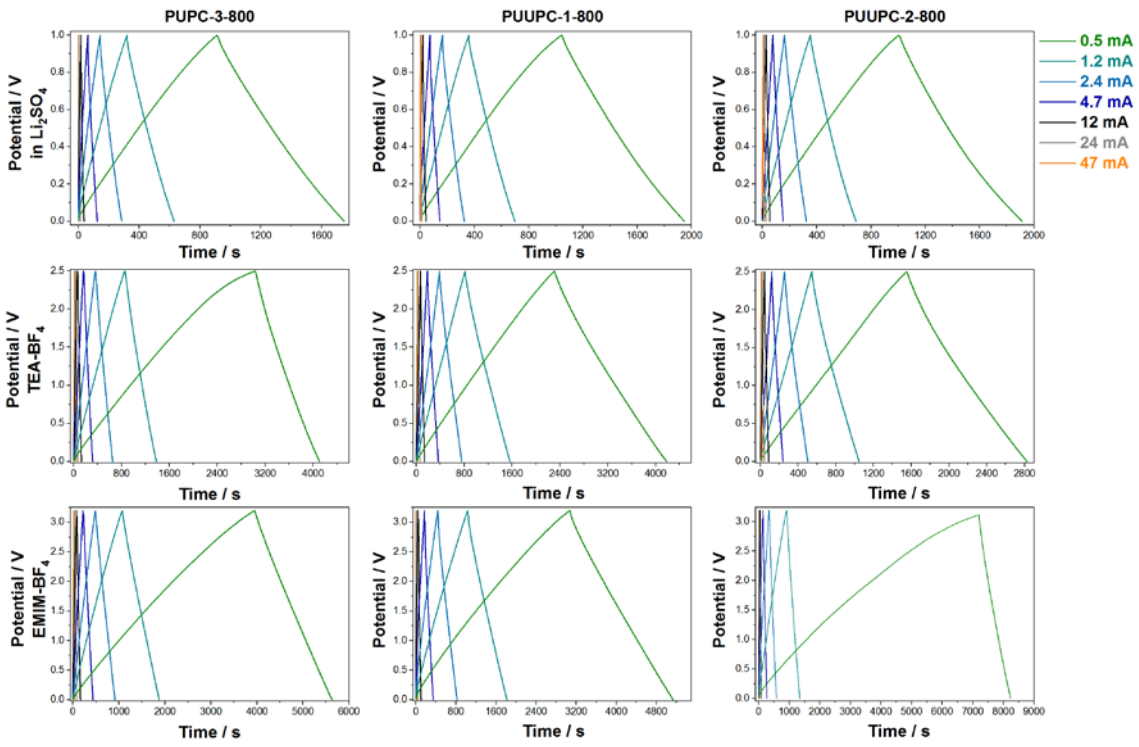

Figure S10: Galvanostatic cycling with potential limitation (GCPL) matrix of samples PUPC-3-800, PUUPC-1-800, and PUUPC-2-800 measured in aqueous electrolyte Li_2SO_4, organic electrolyte TEA-BF_4 in ACN and ionic electrolyte EMIM-BF_4.

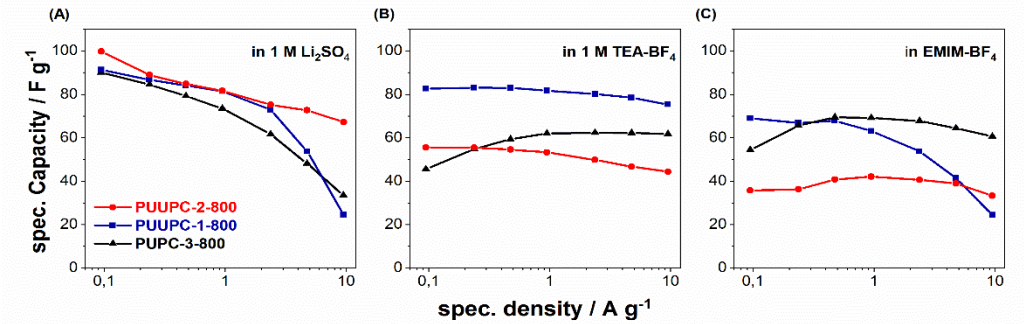

Figure S11: Galvanostatic charge–discharge rate handling plots at different specific current values of the samples PUUPC-800-1 (blue), PUUPC-800-2 (red) and PUPC-800-3 (black) in (A) aqueous Li_2SO_4 electrolyte, (B) organic TEA-BF_4 in ACN and (C) ionic liquid EMIM-BF_4.

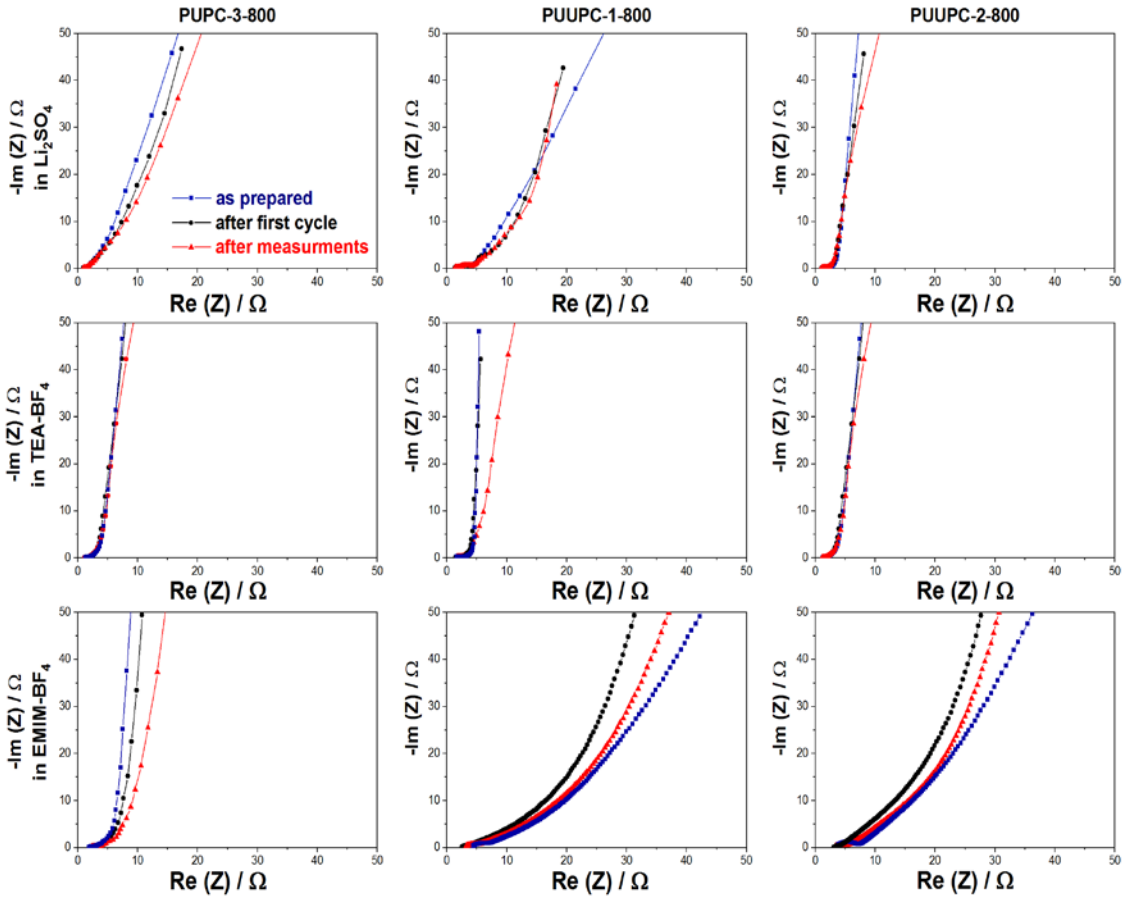

Figure S12: Potential electrochemical impedance spectroscopy (PEIS) matrix of samples PUPC-3-800, PUUPC-1-800, and PUUPC-2-800 measured in aqueous electrolyte Li_2SO_4, organic electrolyte TEA-BF_4 in ACN and ionic electrolyte EMIM-BF_4**.**

S3 Activation mechanism

Mechanism of activation with K_2CO_3 according to McKee et al. [66]:

$$K_2CO_3 + 2\,C \rightleftharpoons 2\,K + 3\,CO$$

$$2\,K + 2n\,C \rightleftharpoons 2\,C_nK$$

$$2\,C_nK + CO_2 \rightleftharpoons (2C_n)K_2O + CO$$

$$(2C_n)K_2O + CO_2 \rightleftharpoons 2\,nC + K_2CO_3$$